RESEARCH ARTICLE

Detection and Mapping of Kochia Plants and Patches Using High-Resolution Ground Imagery and Satellite Data: Application of Machine Learning

MUHAMMAD HAMZA ASAD[ID]**¹, (Student Member, IEEE), SAJID SALEEM²,
AND ABDUL BAIS**[ID]**¹, (Senior Member, IEEE)**

¹Electronic Systems Engineering, Faculty of Engineering and Applied Science, University of Regina, Regina, SK S4S 0A2, Canada
²Department of Computer Science, National University of Modern Languages, Lalazar, Rawalpindi 46000, Pakistan

Corresponding author: Abdul Bais (abdul.bais@uregina.ca)

ABSTRACT The presence of Kochia weed is harmful to crop production. It can grow well in harsh conditions and is resistant to common herbicides like glyphosate. It causes stress to crops and spreads quickly, forming large patches. Early detection of Kochia is crucial for its effective control. However, it is challenging to detect Kochia due to its close resemblance with early-stage crops. As Kochia seeds are water and air-borne, these can also spread in the field from neighbouring farms. Therefore, Kochia needs to be managed both at the field as well as regional levels. Currently, object-based detection methods are used for Kochia detection at the field level, but there is still a lack of literature on mapping Kochia at a regional level. Our research proposes a methodology for accurately detecting, localizing and quantifying Kochia plants in fields using high-resolution RGB imagery. We also explore the potential of detecting Kochia patches at a regional level using satellite imagery. Our approach uses semantic segmentation techniques to process geotagged RGB images, allowing us to identify and quantify individual Kochia plants in the field. To ensure accurate detection, we have established a minimum Kochia density threshold based on the density of Kochia in RGB images. This threshold enables us to distinguish the spectral signature of satellite imagery pixels containing a high density of Kochia. We label the satellite imagery based on the geo-locations where Kochia density exceeds the threshold value. Our method has a 99% accuracy rate in detecting Kochia patches using multi-spectral satellite imagery with a density threshold of 40%. The semantic segmentation model trained on RGB imagery for in-field mapping has a mean intersection over union value of up to 0.8606. These results suggest pixel-level Kochia segmentation of satellite imagery can be performed more accurately if a pixel has more than 40% Kochia mix. Our study highlights the potential of using high-resolution RGB imagery and satellite data at the farm and regional levels for effective Kochia management. Detecting Kochia early and accurately can help prevent crop damage and ensure successful crop production.

INDEX TERMS Kochia patch detection, machine learning, remote sensing, semantic segmentation.

I. INTRODUCTION

Kochia (Kochia scoparia) is one of western Canada's most common weed problems [1]. It is a highly invasive weed.

The associate editor coordinating the review of this manuscript and approving it for publication was Yizhang Jiang[ID].

It has an extensive root system, which can extend up to a radius of 2.4m, helping it absorb moisture and nutrition from soils even in harsh soil and weather conditions [2]. It competes with crops for soil nutrients, significantly impacting crop yield. The intensity of competition varies, as some crops experience moderate competition while others face strong

competition. For instance, wheat crops can suffer up to a 60% yield reduction with 240-520 Kochia plants per square meter. In comparison, Sugarbeet crops are highly susceptible and experience yield reductions of 78%-95% with just three Kochia plants per square meter [3]. Kochia's invasiveness is compounded by its highly prolific characteristics. It produces up to 120,000 seeds per plant [4]. Kochia seeds spread through wind-blown broken plants in the fall season, forming large patches of Kochia in successive crops [5]. Additionally, Kochia is known for its tolerance to abiotic stresses. It can thrive in challenging soil conditions, such as saline, dry, and extreme pH soils, resulting in further yield losses in low-potential soils [4]. These characteristics of Kochia help it thrive outside of its native habitat. Kochia also has a reputation for developing herbicide resistance. It has developed resistance to Photosystem II (PSII) inhibitors, Acetolactate Synthase (ALS) inhibitors, glyphosate, and synthetic auxins herbicides over time [6], [7], which further complicates the control strategies for Kochia management. Some mechanical and chemical methods have been developed to control Kochia [8], [9]. Mechanical methods such as soil tillage before crop seeding are commonly used, though not aligned with no-tillage and eco-friendly agricultural practices [10]. Pre-emergent herbicide application is also a commonly used chemical method for Kochia control, but it can sometimes stress the crop [11].

In short, identifying and locating Kochia early on is crucial for effective control as it is a hardy plant that can spread rapidly and develop herbicide resistance. However, this can be challenging as it closely resembles crops in their early stages [6]. Various methods are available for detecting Kochia in the field, but a comprehensive approach is necessary to manage its spread. This involves the use of remote sensing satellite imagery to map Kochia both within and beyond field boundaries. This approach can help make decisions at the regional level regarding Kochia management.

Various methods for detecting weeds using remote sensing technology, including supervised object-based and pixel-based techniques [12] exist. Object-level classification requires high spatial resolution imagery to extract plants' morphological and texture features. This can be achieved through Unmanned Aerial Vehicle (UAV) imagery, but it is not scalable for larger areas. On the other hand, satellite imagery is scalable and can be used for pixel-based segmentation. The accuracy of pixel-based methods is limited by the heterogeneity of pixels, as they may contain multiple features like soil, crop, and weed in a single pixel [13].

This paper introduces a hybrid approach to detecting individual Kochia plants and patches using high-resolution ground imagery and remote sensing satellite data. By limiting the heterogeneity of pixels to a threshold, this methodology improves the pixel-level classification accuracy of remote sensing satellite imagery. The study leverages the recent success of semantic segmentation in accurate weed detection using geo-referenced high-resolution RGB image samples to generate a Kochia density map [14], [15], [16], [17], [18],

[19], [20]. The generated map is then compared with corresponding satellite imagery to identify the optimal Kochia density threshold. This threshold ensures that the spectral signature of Kochia patches is distinctive enough to be detected from satellite imagery.

We compare the performance of ResNet50-SegNet and ResNet50-UNet models and find that ResNet50-SegNet achieves a higher mean Intersection Over Union (mIOU) of 0.8606, compared to ResNet50-UNet's mIOU of 0.7837. By using semantic segmentation, we can generate a Kochia density map for the field. Through our analysis, we determine that a minimum Kochia density threshold of 40% is necessary for heterogeneous pixels to be labelled as belonging to Kochia patches. We identify locations with Kochia density above 40% as likely Kochia patches and label these locations on satellite imagery accordingly.

To develop the Kochia patch detection model, we train and evaluate an Artificial Neural Network (ANN) using four fields of Canola and Oats. The ANN model uses 8-band satellite data as predictor variables and the Kochia patch as the target variable. Our trained ANN achieves a test accuracy of 99% and a low test loss of 0.0016. Two primary factors contributed to our ability to achieve greater accuracy in detecting Kochia patches. Firstly, we applied a threshold to account for the varying characteristics of satellite imagery pixels. Secondly, our research focused on Oats and Canola fields, as we possessed high-resolution ground imagery that included Kochia infestations for these two crops. To improve the applicability of our model, it is necessary to acquire Kochia infestation data for other crops and vegetation types. Nevertheless, our current model effectively detects Kochia patches in Oats and Canola fields using multispectral satellite imagery. This proposed methodology has important implications for effective Kochia management strategies, allowing for timely detection and control of this invasive weed, thereby reducing its impact on crop yield and minimizing the need for herbicide use.

To our knowledge, we do not find any work in literature where the Kochia patch is detected using satellite imagery. Also, semantic segmentation is applied for the first time to detect, localize and quantify Kochia in high-resolution ground images for in-field mapping of Kochia density. The paper makes the following contributions:

1) We propose a methodology for detecting, localizing and quantifying individual Kochia plants at the field level using semantic segmentation.
2) We determine the minimum Kochia density threshold of 40% for heterogeneous pixels to have distinct spectral signatures in Oats and Canola crops.
3) We develop a method for Kochia patch detection using satellite imagery and high-resolution ground imagery.

The remainder of the paper is organized as follows: Section II presents the literature survey, Section III details the proposed methodology, Section IV discusses results, and Section V includes conclusions and recommendations for future work.

II. RELATED WORK

In the literature, three types of research are reported on detecting and controlling Kochia. The first type is focused on identifying Kochia weeds, in general, alongside other plants. The second type differentiates between herbicide-susceptible and herbicide-resistant Kochia, while the third concentrates on Kochia's response to soil and the environment.

To identify Kochia plants in general, object-level classification techniques are employed to distinguish them from other weed and crop plants. Various methods have been utilized, including Support Vector Machines (SVM), neural networks, and deep neural networks like VGG16 [21]. For example, Sunil et al. have developed a classification system for four weeds (Horseweed, Kochia, Ragweed, and Waterhemp) and eight crops (black Beans, Canola, Corn, Flax, Soybean, and Sugarbeet) utilizing texture features extracted from RGB images. They have compared the performance of SVM and VGG16 and have achieved 90% and 95% accuracy for Kochia using SVM and VGG16, respectively [22].

Another study by Judit et al. employ optical sensor data to map Kochia, Russian thistle, and prickly lettuce post-harvest. They achieve an accuracy of 78.1% by detecting greenery in the data during grain flow, which is geo-referenced and corresponds with the pre-harvest and post-harvest ground truth maps constructed by experts for the three weeds [23]. However, these methods only classify images to identify if they contain Kochia or not and do not quantify the extent of Kochia infestation in the images. To accurately ascertain the spread of Kochia, it is essential to localize and quantify the infestation.

The second work found regarding Kochia is detecting and classifying herbicide-susceptible and herbicide-resistant Kochia plants. Agronomists need to perform tailored herbicide prescriptions for Kochia. Traditional methods to distinguish Kochia susceptible and Kochia resistant involve lab-based dose-response assays and shoot bio-assays, which are time-consuming and tedious. To speed up this process, hyperspectral imaging is used. Paul et al. can distinguish between Kochia and crop and classify herbicide-susceptible and herbicide-resistant Kochia with accuracies of 67%, 76%, and 80% in field conditions using hyperspectral imaging [24]. Baryan et al. compare the performance of ground-based and Unmanned Aerial System (UAS) based hyperspectral imagers and achieve accuracies up to 80% using SVM. It improves to 99% using neural networks. However, they observe that the ground-based hyperspectral imagery is more accurate than the UAS-based one [25]. Alimohammad et al. used a thermal sensor to distinguish between herbicide-resistant and herbicide-susceptible Kochia, achieving a maximum accuracy of 86% with a kappa coefficient of 0.77 using various algorithms like maximum likelihood classification, spectral angle mapper, SVM, and decision tree [26]. However, hyperspectral sensors are expensive and not feasible on a commercial scale for detecting Kochia in the first place and then sub-classifying it as herbicide-resistant and herbicide-susceptible.

The third type of study for Kochia management leverages Kochia germination and its response to environmental and soil conditions. They suggest exploiting these properties for the effective management of Kochia. Timothy and Rene study Kochia emergence in North America and find that Kochia seeds at shallower soil depths have a higher probability of germination than those at deeper soil depths [27]. This suggests that seed burial depth plays an important role in Kochia germination. Anita et al. conducted a Kochia seed viability study in North America and found that Kochia seed persistence decreases significantly if the seeds are buried for more than two years [28]. The study suggests using tillage and crop cover to bury Kochia seeds deep inside the soil as a potential control strategy. Derek et al. study the impact of soil properties on herbicide effectiveness on Kochia and find that Kochia can germinate in low-moisture soils, which can complicate herbicide efficacy [29]. This finding suggests that understanding the environmental conditions for Kochia germination can inform more effective herbicide application. Bilquees et al. study Kochia as a fodder crop and found that it was tolerant to saline soils during both the germination stage and growth [30]. Similarly, NS et al. study different Kochia varieties for salinity tolerance and find that Kochia scoparia is more tolerant to salts than Kochia prostrata [31].

The above research studies emphasize the significance of soil properties in understanding the spatial distribution of Kochia in the field. However, high-resolution mapping of soil properties is required beyond field boundaries for using these properties for Kochia management at the regional level. Alternatively, the ever-increasing spatiotemporal resolution of remote sensing satellite data can be exploited for identifying potential Kochia infestation beyond the boundaries of agriculture fields. Integrating in-field and regional Kochia patch detection presents a significant opportunity to develop more effective and efficient Kochia management strategies.

This paper develops a methodology to detect individual Kochia plants and patches using high-resolution ground imagery and remote sensing satellite data to address the aforementioned gaps and exploit opportunities. This methodology involves machine learning algorithms to detect Kochia plants and patches in high-resolution imagery, which can then be used to develop maps of Kochia distribution at various scales. The following section details the methodology adopted in this study.

III. METHODOLOGY

This section describes detecting individual Kochia plants and patches using high-resolution ground imagery and satellite data. The method involves two main parts: (1) detection and quantification of Kochia in high-resolution ground imagery and (2) detection of Kochia patches using multi-spectral satellite data. All steps of the proposed methodology are listed below:

1) High-resolution geo-tagged RGB image acquisition from fields.

2) Pre-processing of RGB images for labelling Kochia pixels in RGB images.
3) Augmenting the size of the labelled dataset
4) Training semantic segmentation models
5) Estimating Kochia density in each image
6) Mapping Kochia density on the map
7) Multispectral satellite image acquisition [32] of the same fields, temporally as close as possible to the day of RGB image acquisition
8) Comparing different Kochia densities obtained from in-field Kochia density mapping with satellite imagery to find the minimum Kochia density threshold whose spectral signature is distinctive
9) Labelling satellite imagery pixels as Kochia patches where corresponding in-field Kochia density is above the Kochia density threshold
10) Training ANN model using multispectral satellite bands predictor variables and Kochia patch as the target variable

The flowchart in Fig. 1 explains all the steps in our methodology. The following subsections provide details of the above-listed steps:

A. DATA ACQUISITION

This study uses two types of data: high-resolution ground imagery and remote sensing satellite imagery, with details below.

1) HIGH-RESOLUTION GROUND IMAGERY

Four fields containing Kochia weed are selected in the Canadian Prairies for this study. High-resolution image samples are acquired using a camera mounted on ground-moving farm equipment. The camera captures RGB images in a $50' \times 70'$ grid pattern. The dimension of each image is 1440×1080 pixels. The data is provided by Croptimistic Technology Inc. [33]. Data for three fields was collected in 2022, and for the fourth field, the data was collected in 2021. These fields are located in Saskatchewan, Canada. Table 1 summarizes the images collected from each field. Names and exact locations of the fields are anonymized.

TABLE 1. High-resolution RGB images acquired through ground moving equipment.

Field	Number of Acquired Images
Field-1	1970
Field-2	2724
Field-3	699
Field-4	602

2) SATELLITE IMAGERY

Satellite imagery with 0% cloud cover is acquired from PlanetLabs' Planetscope satellite with a ground sample distance of $3m$ per pixel [32]. The satellite imagery used in this study consists of eight bands: Coastal Blue (443 nm), Blue (490 nm), Green-I (531 nm), Green (565 nm), Yellow (610 nm), Red (665 nm), Red Edge (705 nm) and NIR (865 nm). The eight-band satellite imagery is collected by Super Dove (SD) sensor mounted on the Planetscope satellite. Two new bands, Yellow (610 nm) and Green-I (531 nm) are added to SD sensor data. The remaining six bands have equivalent available in Sentinel-2 [34]. Care has been taken to download satellite imagery temporally as close as possible to the day of ground image acquisition. Figure 2 shows high-resolution image sample geo-locations overlaid on respective satellite imagery to illustrate the spatial relationship of the two above-mentioned datasets.

B. SEMANTIC SEGMENTATION

In this study, we use semantic segmentation on RGB ground images to detect, localize and quantify Kochia infestation. We employ SegNet [35] to train semantic segmentation models due to fewer training parameters involved as compared to the state-of-the-art deep learning architectures like [19], [36], and [37]. To compare the performance of both networks on Kochia, ResNet50 [38] is used as the encoder block for feature extraction. ResNet50 deals with the problem of vanishing gradients in deep networks during back-propagation by using identity skip connections [39]. Adadelta [40] is used as the optimizer, and models are trained for 150 epochs. To prepare RGB images for training, pixel-level labelling of Kochia plants is performed using the Segments.ai tool [41]. We labelled 124 high-resolution ground images at the pixel level for Kochia plants. Then we randomly split the data into 80-20% training (99) and test (25) images. As deep learning requires large data to train a well-generalized model, we increase the training data size using augmentation methods like random rotation, horizontal and vertical flipping, scaling and blurring to mimic the real field conditions. Using augmentation methods, we increase the training data size to 10 times. Before training the model, we again randomly split augmented images into 85-15% training and validation data. Validation data is used at the end of every training epoch to evaluate model fit on training data.

After training the semantic segmentation model, predictions are made for all images in the field and Kochia density given by the following equation is estimated for each image.

$$Kochia\ Weed\ Density = \frac{Kochia\ leaf\ pixels\ in\ image}{Total\ pixels\ in\ image}$$

Using this data, the in-field Kochia density map is generated.

C. KOCHIA PATCH DEFINITION

Through our research, we have established the minimum Kochia density threshold required to detect a Kochia patch. We accomplished this by comparing the spectral signature of Kochia to other vegetation at different densities. If an RGB image has a Kochia density that exceeds the threshold value, then it's probable that a Kochia patch is present at that geo-location. This patch can be detected through remote sensing satellite data, which has a unique spectral signature. To determine this threshold, we plotted the spectral signature
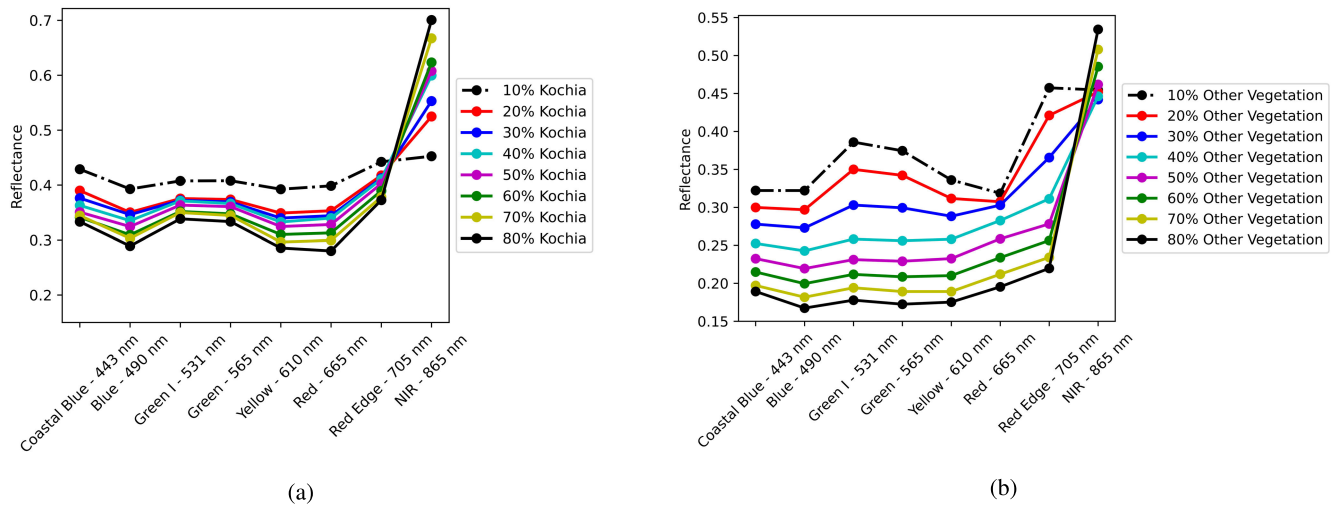
FIGURE 1. Flowchart for kochia plants and patch detection.

(a)   (b)

FIGURE 2. (a) Field-1 and (b) Field-2, RGB image sample points overlayed over satellite imagery.

of Kochia and other vegetation against the eight bands of satellite imagery. Figure 3a portrays the spectral signature of Kochia at varying percentages of Kochia densities in images. As the Kochia densities grow, the transition from Red to Red Edge to NIR becomes more distinct. Similarly, reflectance sharply rises from Blue to Green-I and then falls more sharply towards the Yellow band as Kochia densities increase. The spectral signature becomes more distinct as Kochia densities increase. It's worth noting that when calculating Kochia reflectance at different densities, the remaining content of that pixel is non-vegetation, such as soil or crop residue. For instance, if Kochia density is estimated at 40% in a pixel,

the remaining 60% of the pixel is non-vegetation (soil, crop residue, etc.).

Fig. 3b shows the spectral signature of non-Kochia vegetation at varying densities for comparison with the Kochia spectral signature. For higher vegetation densities (30% to 80%), there is a gentle slope of reflectance rise from Coastal Blue towards Red Edge. However, it sharply rises from Red Edge to the NIR band. Same as in the Kochia case, non-Kochia vegetation's spectral signature is calculated for the locations where there is only non-Kochia vegetation, and the remaining part of the pixel is non-vegetation (soil, crop residue etc.).

FIGURE 3. (a) Spectral signature of kochia at varying densities and (b) spectral signature of other vegetation at varying densities.

Although Kochia is undesirable even in small amounts, it can be challenging to distinguish its spectral signature in satellite imagery due to limited spatial resolution. Figure 4a shows error bars demonstrating this difficulty, with the 10% Kochia bar representing the mean reflectance of pixels where Kochia density is greater than 10%, while the remaining pixels contain non-vegetation content. Similarly, the 10% vegetation bar represents the mean reflectance of pixels where other vegetation is greater than 10%, and the remaining pixels contain non-vegetation content. The difference in spectral signature between 10% and above Kochia and 10% and above other vegetation is not distinctive. However, as Kochia and other vegetation densities increase, the spectral signature difference between the two increases, as shown in Figure 3. At 50% density, for example, the reflectance of other vegetation does not show significant changes from Coastal Blue to Red bands. In contrast, the reflectance of Kochia increases from Blue to Green-I before dropping from Green to Yellow. The transition from Red to Red Edge is also a sharper rise for Kochia than other vegetation. Nonetheless, both Kochia and other vegetation exhibit a sharp increase in reflectance from Red Edge to NIR, making them distinguishable from the non-vegetation spectral signature of soil and dead crop residue. It is worth mentioning that the high standard deviation in error bars is due to the density threshold selecting a range of all densities above the threshold. For instance, the 10% Kochia density threshold includes all Kochia densities above 10%.

By examining Figure 3a and Figure 3b, we notice that the spectral differences between Kochia and other vegetation types are inconsistent until they reach a density of 30%. Once the density reaches 40% or more, the spectral differences between Kochia and other vegetation become noticeable and consistent. As a result, we have determined that 40% is the minimum Kochia threshold for labelling potential Kochia patches in heterogeneous satellite pixels. In the next

subsection, we will train ANN models for various Kochia density thresholds.

D. DETECTING KOCHIA PATCH

We use ANN to map the non-linear relationship between the predictor and target variables. It has an input layer, three hidden layers, and an output layer. The input to the network is a stack of eight bands of satellite imagery. Several ANNs are trained for varying definitions of the Kochia patch to compare their performance. Table 2 summarizes the hyper-parameter settings for the ANNs, which include the learning rate, number of epochs, batch size, activation function, and number of neurons in each hidden layer. The hyper-parameters are important for the performance of the ANN and are chosen based on experimentation and optimization.

TABLE 2. Hyperparameter settings for ANN.

Parameter	Values
Layer1	32
Layer2	64
Dropout Rate	30%
Activation Function	ReLU
Optimizer	Adam
Loss Function	Binary Crossentropy

IV. RESULTS DISCUSSION

The proposed method is tested on four different fields. In the first step of this methodology, we apply semantic segmentation to estimate the density of Kochia in high-resolution ground imagery. This is the ground truth information for detecting Kochia patches using satellite imagery. Our previous work in [18] and [42] forms the basis for this semantic segmentation. Previous studies have shown that SegNet, with ResNet-50 as the encoder block, performs better than other semantic segmentation architectures. To verify this, we train and compare the performance of SegNet with other
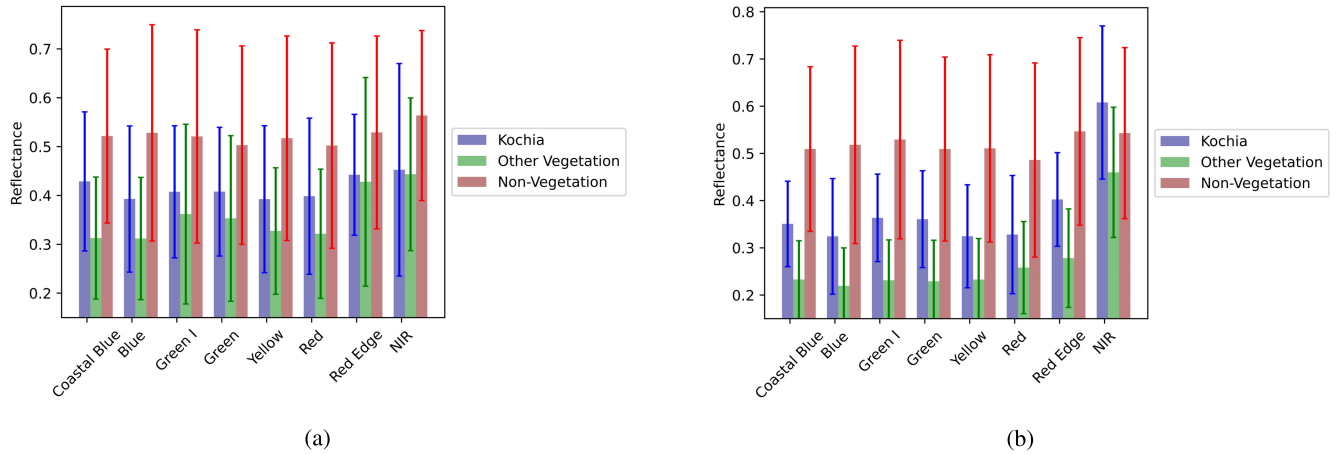
FIGURE 4. (a) Spectral signature of 10% Kochia, 10% other vegetation and 90% non-vegetation and (b) Spectral signature of 50% Kochia, 50% other vegetation and 50% non-vegetation.

TABLE 3. Summary of Kochia semantic segmentation models performance.

Model	IOU Kochia	IOU Non-Kochia	mIOU	fwIOU
ResNet50 - FCN32 [43]	0.5000	0.9550	0.7275	0.9217
ResNet50 - PSPNet [44]	0.4969	0.9536	0.7253	0.9201
ResNet50 - SegNet [35]	**0.7791**	**0.9420**	**0.8606**	**0.9120**
ResNet50 - UNet [37]	0.6523	0.9151	0.7837	0.8668
ResNet50 - DeepLab V3+ [36]	0.6738	0.9435	0.8086	0.9032

architectures setting ResNet50 as the encoder block. We evaluate trained models using class-wise Intersection over Union (IOU), mean IOU (mIOU), and frequency-weighted IOU (fwIOU). We use IOUs to discount the class imbalance problem that may arise while evaluating models. The ratio of foreground and background varies from 0 to 98%. In such a scenario, accuracy as a classification metric can be misleading. However, IOU evaluates models based on the overlap of the predicted segment and ground truth segment, which is less prone to class imbalance problems. The following expressions give IOU metrics:

$$\text{IOU} = \frac{\text{Area of Overlap}}{\text{Area of Union}} = \frac{p_i \cap g_i}{p_i \cup g_i} \quad (1)$$

p is the predicted class and g is the ground truth label. To compute semantic segmentation's overall performance mean of IOUs is also estimated as provided by the following equation:

$$\text{mIOU} = \frac{IOU_i + IOU_j}{2} \quad (2)$$

where i and j are two classes of pixels. In our case, one is Kochia, and the other is non-Kochia. To account for class imbalance in evaluating model performance, fwIOU is used, which assigns weight to each class based on its frequency in the dataset.

$$\text{fwIOU} = w_i \times IOU_i + w_j \times IOU_j \quad (3)$$

where w_i and w_j are the weights of the respective classes.

Table 3 presents these IOU metrics for the trained ResNet50-SegNet model. It is observed that SegNet outperforms all other semantic segmentation architectures, with UNet being the second-best-performing network. It agrees with our previous findings for Canola and Oats crop detection and quantification [17], [42]. It is also noteworthy that SegNet requires less memory and computational power than UNet and DeepLab V3+ due to less trainable parameters [19].

Figure 5 shows the performance of a semantic segmentation model for detecting Kochia in different types of crops. Figure 5a consists of only Kochia and some soil pixels. The model detects Kochia with a weed density of 98%. Figures 5c and 5d refer to the case when Kochia, crop (Canola in this case) and non-vegetation pixels are present in the image. The model successfully detects Kochia, and 48% density is estimated despite natural light and soil colour variations between Figure 5a and Figure 5c.

The model's performance suffers when detecting occluded Kochia within narrow-leaf crops, as shown in Figure 5e. This challenge arises from altered lighting conditions, changed soil colour, and the presence of multiple plants in close proximity. Figure 5e highlights five scenarios illustrating the model's performance. In the first case, Kochia and non-Kochia weeds are both labelled as Kochia due to their resemblance, especially during Kochia's mid-growth stage.

The second case involves false positives, where Oats and other weeds are misclassified as Kochia due to shape variations. Similarly, the third case sees a narrow-leaf weed misidentified as Kochia. The model handles lighting and soil changes well, focusing on leaf shape features rather than colour. However, it struggles with close shape resemblances. In the fourth case, a non-Kochia weed is correctly identified, despite some resemblance, unlike in the first instance.
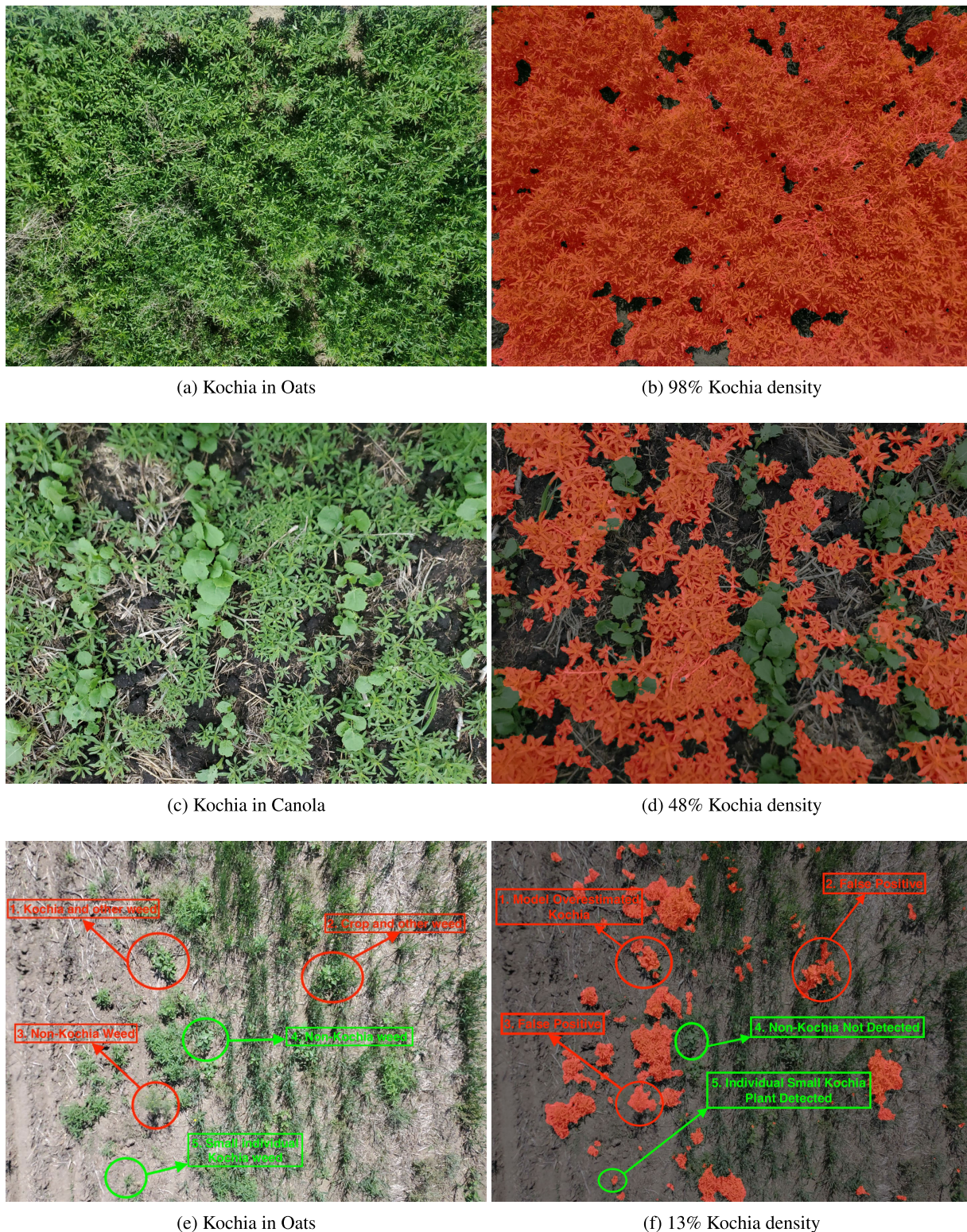
(a) Kochia in Oats

(b) 98% Kochia density

(c) Kochia in Canola

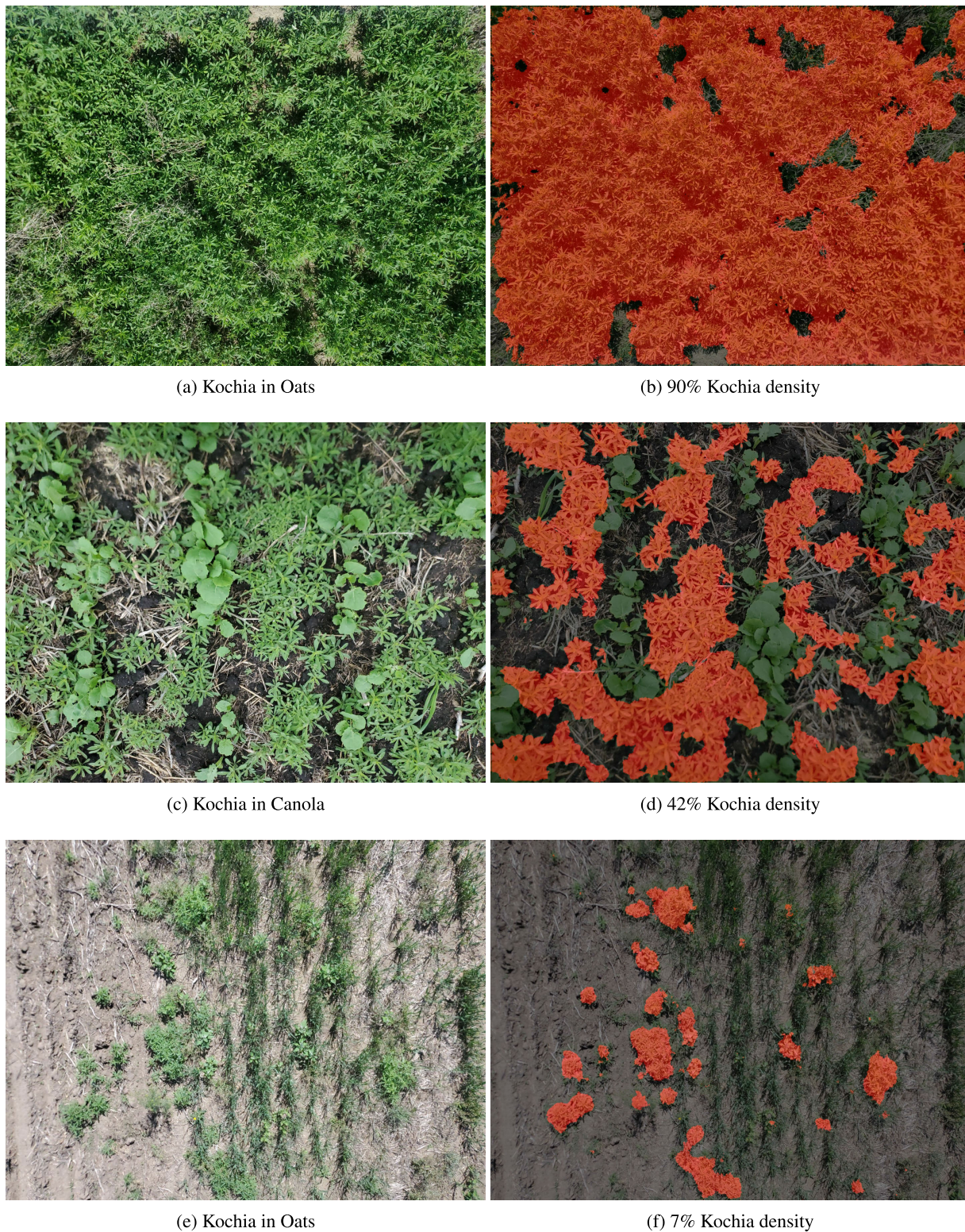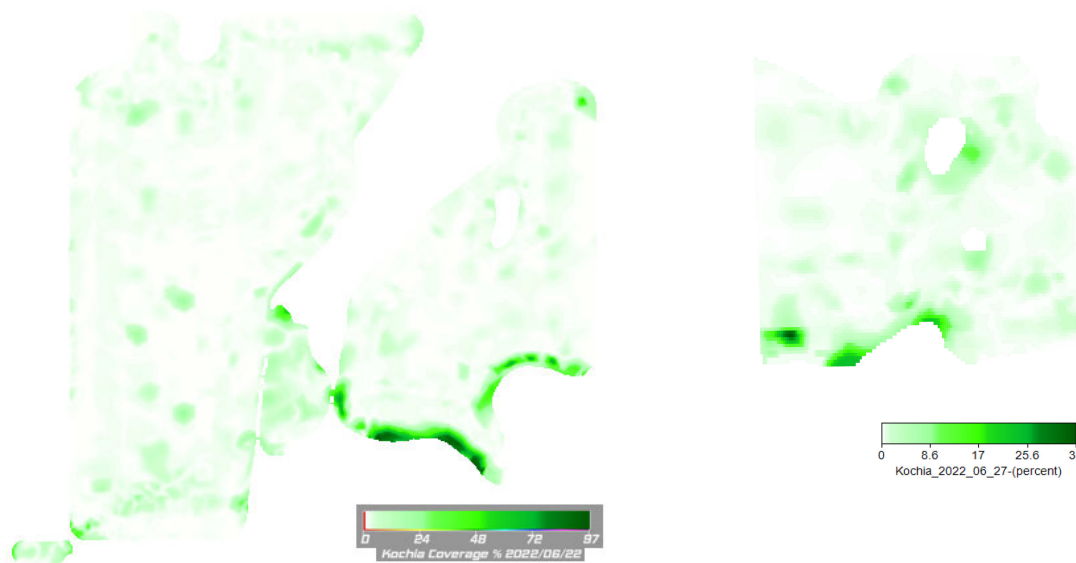(d) 48% Kochia density

(e) Kochia in Oats

(f) 13% Kochia density

FIGURE 5. ResNet50 - SegNet performance for kochia detection, localization and quantification at variable Kochia infestation levels.

This semantic segmentation model is designed to detect individual Kochia plants, which is crucial for preventing rapid field spread. Even small Kochia plants are successfully detected in the fifth case. However, the ResNet50-based UNet performs poorly in Kochia detection, as seen in Figure 6. It shows predictions on the same test images as in Figure 5.

(a) Kochia in Oats

(b) 90% Kochia density

(c) Kochia in Canola

(d) 42% Kochia density

(e) Kochia in Oats

(f) 7% Kochia density

FIGURE 6. ResNet50 - UNet performance for kochia detection, localization and quantification at variable kochia infestation levels. UNet underpredicts Kochia compared to SegNet, resulting in 6%-8% less Kochia density estimation.

The ResNet-UNet model only partially detects some Kochia plants, leading to a 6% to 8% underestimation in Kochia density.

Figure 7a and Figure 7b illustrate the mapping of Kochia in Field-1 and Field-3 using the predictions from the semantic segmentation model. Figure 7a shows that

(a) Kochia density map for Field-1

(b) Kochia density map for Field-3

FIGURE 7. Comparing Field-1 and Field-3 kochia density maps using semantic segmentation applied on high-resolution ground images.
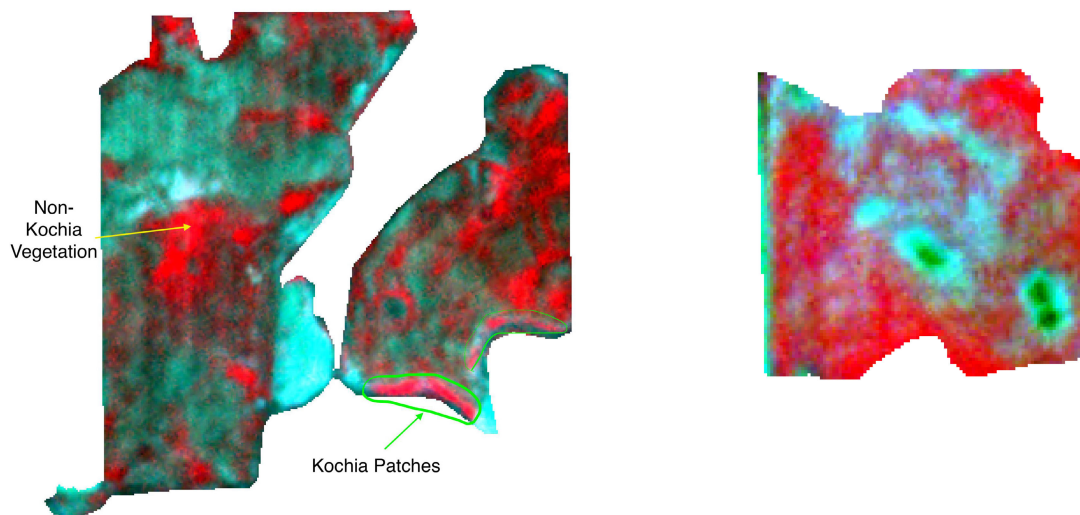

(a) False colour composition of Field-1 [32]

(b) False colour composition of Field-3 [32]

FIGURE 8. Comparing Field-1 and Field-3 where NIR is represented by Red channel, Red by Green Channel and Green by Blue Channel, the false colour composition of satellite imagery.

a higher density of Kochia weed is present across the southern fringes of the field, characterized by low-lying depressions and saline soils. In such harsh soil conditions, crops compete poorly with Kochia, resulting in a higher weed cover. Similarly, in Field-3, Kochia is also prevalent across the low-lying edges of the field. However, Kochia density is low in Field-3, where it stays less than 40%.

Figure 8a depicts false-colour composite satellite imagery of Field-1 using NIR, Red, and Green bands to visualize the correspondence with Figure 7a. Comparing the two figures, a correlation can be observed at the southern fringes of the field where highly dense Kochia patches exist. Locations with a higher density of Kochia weed in ground images are visible in satellite imagery, which agrees with Figure 3. Moreover, it can be observed that the reflectance values for the NIR
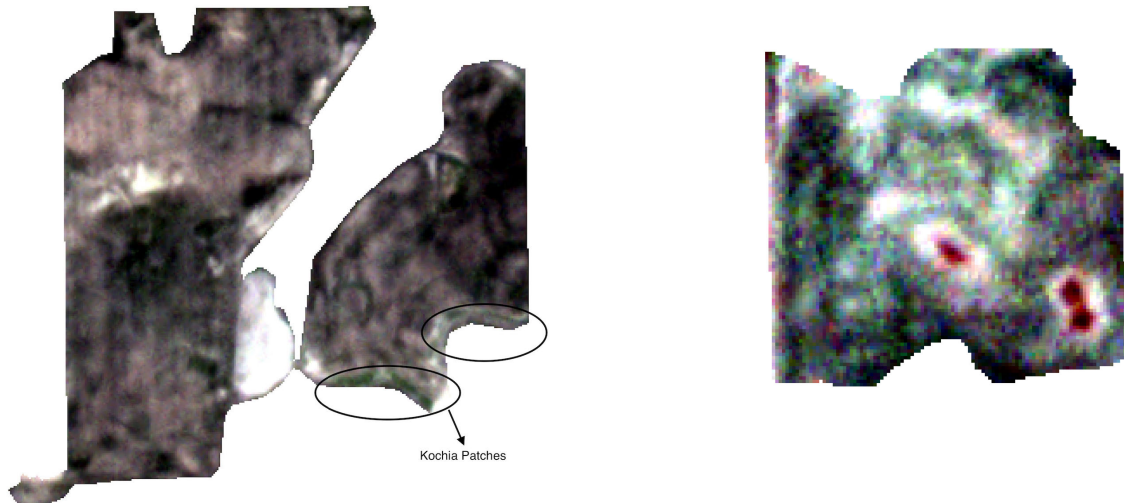
(a) Differences between Kochia and Non-Kochia in Field-1 [32].

(b) Diminishing differences between Kochia and Non-Kochia in Field-3 [32].

FIGURE 9. Comparing Field-1 and Field-3 where Yellow - 610 nm represented by Red Channel, Green - 565 nm represented by Green Channel and Green I - 531 nm represented by Blue Channel.

band are higher for Kochia than other vegetation. However, in Figure 8b, we do not observe a strong correlation with Figure 7b. There is vegetation along the edges of the fields, but Kochia percentages are less than 40%. We observe that the spectral signature of Kochia percentages less than 40% is not distinctive from non-Kochia vegetation.

In Figure 3, it is observed that there are differences in the reflectance values of Green-I, Green and Yellow bands between Kochia and other vegetation. To further visualize the spectral signature of Kochia, Figure 9a represents the Yellow, Green, and Green-I bands using the Red, Green, and Blue channels, respectively. By comparing Figure 7a and Figure 9a, it can be seen that the Kochia patch is distinctive at the southern fringes of Field-1. This can be attributed to two reasons: Firstly, non-Kochia vegetation is weak during the early crop growth stage, while Kochia is well-established in hard soils such as saline and wet depressions. Secondly, Kochia has a distinctive spectral signature compared to other vegetation for the 8-band multispectral satellite data mentioned above. However, the locations of ground images with low-density Kochia weed are not visible on satellite imagery due to the limitations of the ground spatial resolution of satellite imagery. It is verified from Figure 9b that low-density Kochia patches are not easily distinguishable from non-Kochia vegetation.

Based on the aforementioned observations, we trained an ANN binary classifier model to predict Kochia patches using 8-band multispectral satellite imagery as the predictor variable and Kochia patch as the target variable. In this regard, the dataset is divided into an 85%-15% ratio for training and test purposes. There are 5005 instances in the training set and 900 instances in the test set. The training set is further
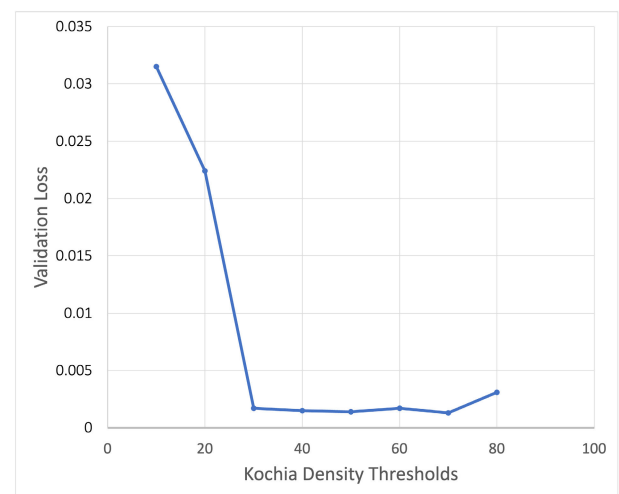

FIGURE 10. Validation losses of ANN models for different kochia thresholds.

divided into 80% training and 20% validation sets. Table 4 summarizes the results of the ANN model. We train the ANN models for different Kochia density thresholds. We find that 40% is the optimal threshold value for Kochia patch density detection using satellite imagery. Figure 10 shows the validation losses plotted against different threshold values of Kochia density. It can be observed that the validation loss of the ANN model is higher for 10% and 20% density thresholds, which highlights the limitation of the spatial resolution of satellite data in detecting small Kochia patches. However, after 30% density, the loss remains low with small variations.

After analyzing Figures 3 and 10, we have chosen a threshold value of 40% to distinguish between pixels

TABLE 4. ANN model performance for kochia patch detection.

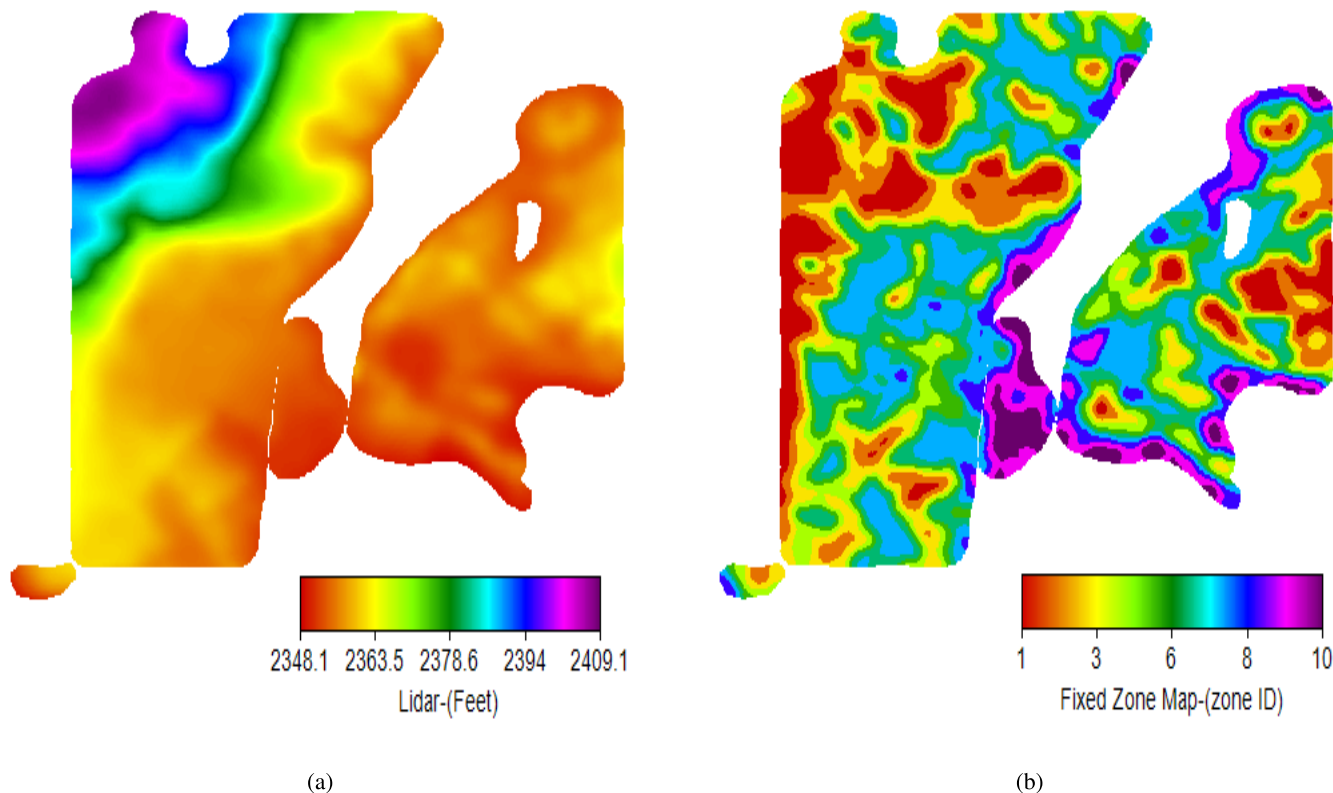| Kochia Density Threshold	Training Loss	Training Accuracy	Test Loss	Test Accuracy
10%	0.039	64%	0.040	53%
30%	0.021	76%	0.002	77%
40%	0.0136	99%	0.0016	99%
70%	0.0132	99%	0.0015	99%

(a)

(b)

FIGURE 11. Field-I: (a) Elevation Map and (b) SWAT map.

containing Kochia patches and pixels containing individual Kochia plants or no Kochia plants, based on the 40% Kochia threshold, satellite imagery pixels are labelled as indicative of the Kochia patch (1) or not (0). After labelling satellite imagery, the ANN model is trained, where eight bands of satellite act as the predictor variable and the Kochia patch as the target variable. The ANN model demonstrates the test accuracy up to 99% and the test loss of 0.0016. These results indicate that Kochia patches in Canola and Oats fields can be detected using satellite imagery. We achieve higher accuracies for Kochia patch detection for two reasons. First, we limit the heterogeneity of satellite pixels based on a minimum Kochia density threshold. Only those pixels are labelled as Kochia patches where Kochia density is above the threshold of 40%. In this case, its spectral signature becomes distinctive to be detected easily. The second reason is that we applied our method to two crops Canola and Oats. For the model to be better generalized, other crops and vegetation types need to be included during training. It is to be noted that individual Kochia plants or low-density Kochia patches (less

than Kochia density threshold) can be accurately mapped only using semantic segmentation applied to high-resolution ground imagery.

We also compare mapped Kochia density with soil characteristics like elevation and Soil, Water and Topography (SWAT) maps. SWAT maps classify soils into ten zones based on topography, electrical conductivity, moisture content and water flow patterns. Zone 1 is eroded hills, dry and low in organic matter, whereas Zone 10 is wet depressions with higher salt content. Comparing Figure 7a with Figure 11a, we observe that Kochia exists in low-lying southern fringes of the field with higher densities. It is also verified by Figure 11b. In Zone 9 & 10, where the soil is saline and wet, posing harsh conditions for crops to thrive, we find higher Kochia densities. Our observations agree with other research studies found in literature [28], [45]. This finding presents an opportunity to use soil properties like elevation, electrical conductivity, soil organic matter and soil texture in addition to satellite imagery for high-density Kochia patch detection. However, for this purpose, we need to have high

spatial resolution soil properties information at the regional level.

V. CONCLUSION

This study focuses on Kochia, a weed that spreads quickly and is resistant to herbicides, thus competing with crops for nutrients. Our research aims to detect individual Kochia plants using high-resolution ground imagery and map Kochia patches using satellite imagery. The study's results show that ResNet50-SegNet semantic segmentation can detect individual Kochia plants with an IOU of 0.78, mIOU of 0.8606, and fwIOU of 0.92. However, the model's performance may deteriorate when Kochia overlaps or occludes crop rows. We compared various semantic segmentation architectures on Kochia data and found that SegNet outperforms others in terms of IOUs. We used satellite imagery to train a Kochia patch detection model for fields where high-resolution ground imagery is unavailable by defining Kochia patches based on Kochia densities in high-resolution ground images. Through experimentation, we found that labelling satellite imagery for Kochia patches with 40% Kochia density provides the best results. Using 8-band multispectral satellite data as predictor variables and Kochia patches as the target variable, our trained model achieves accuracies up to 99%. We conclude that Kochia patches above 40% Kochia can be detected from multispectral satellite imagery with $3m$ ground spatial resolution. However, to detect Kochia below 40%, higher than $3m$ spatial resolution is required. Our study highlights the potential of using high-resolution RGB imagery and satellite data to detect Kochia at both farm and regional levels accurately. This proposed methodology can contribute to integrated weed management practices and sustainable agriculture by mapping Kochia beyond the field's boundaries. The farmer community can anticipate the spread patterns of Kochia and take preventive measures. However, future research should include soil attributes with satellite data for Kochia patch detection and other crops and vegetation types to develop well-generalized Kochia models.

ACKNOWLEDGMENT

REFERENCES

[1] (2021). *Agriculture Managing Kochia*. [Online]. Available: https://www.gov.mb.ca/agriculture/crops/weeds/print,managing-kochia.html

[2] (2023). *(Kochia Scoparia)*. [Online]. Available: https://fviss.ca/invasive-plant/kochia

[3] C. M. Geddes and S. M. Sharpe, "Crop yield losses due to kochia *(Bassia scoparia)* interference," *Crop Protection*, vol. 157, Jul. 2022, Art. no. 105981. [Online]. Available: https://www.sciencedirect.com/science/article/pii/S0261219422000771

[4] L. F. Friesen, H. J. Beckie, S. I. Warwick, and R. C. Van Acker, "The biology of Canadian weeds. 138. *Kochia scoparia* (L.) Schrad," *Can. J. Plant Sci.*, vol. 89, no. 1, pp. 141–167, Jan. 2009.

[5] H. J. Beckie, R. E. Blackshaw, L. M. Hall, and E. N. Johnson, "Pollen- and seed-mediated gene flow in kochia *(Kochia scoparia)*," *Weed Sci.*, vol. 64, no. 4, pp. 624–633, Dec. 2016.

[6] V. Kumar, P. Jha, M. Jugulam, R. Yadav, and P. W. Stahlman, "Herbicide-resistant kochia *(Bassia Scoparia)* in North America: A review," *Weed Sci.*, vol. 67, no. 1, pp. 4–15, Jan. 2019.

[7] J. Chen, E. Burns, M. Fleming, and E. Patterson, "Impact of climate change on population dynamics and herbicide resistance in kochia *(Bassia scoparia* (L.) A. J. Scott)," *Agronomy*, vol. 10, no. 11, p. 1700, Nov. 2020.

[8] M. F. Diprose and F. A. Benson, "Electrical methods of killing plants," *J. Agricult. Eng. Res.*, vol. 30, pp. 197–209, Jan. 1984. [Online]. Available: https://www.sciencedirect.com/science/article/pii/S0021863484800219

[9] J. S. Petrosino, J. A. Dille, J. D. Holman, and K. L. Roozeboom, "Kochia suppression with cover crops in southwestern Kansas," *Crop, Forage Turfgrass Manage.*, vol. 1, no. 1, pp. 1–8, Dec. 2015.

[10] L. Vincent-Caboud, J. Peigné, M. Casagrande, and E. Silva, "Overview of organic cover crop-based no-tillage technique in Europe: Farmers' practices and research challenges," *Agriculture*, vol. 7, no. 5, p. 42, May 2017.

[11] T. Ehmke, "Weed resistance: Enemy of the plains," *Crops Soils*, vol. 49, no. 1, pp. 20–23, Jan. 2016.

[12] I. L. Castillejo-González, J. M. Peña-Barragán, M. Jurado-Expósito, F. J. Mesas-Carrascosa, and F. López-Granados, "Evaluation of pixel- and object-based approaches for mapping wild oat *(Avena sterilis)* weed patches in wheat fields using QuickBird imagery for site-specific management," *Eur. J. Agronomy*, vol. 59, pp. 57–66, Sep. 2014.

[13] T. Blaschke, G. J. Hay, M. Kelly, S. Lang, P. Hofmann, E. Hofmann, R. Q. Feitosa, F. Van der Meer, H. Van der Werff, F. Van Coillie, and D. Tiede, "Geographic object-based image analysis–towards a new paradigm," *ISPRS J. Photogramm. Remote Sens.*, vol. 87, no. 100, pp. 180–191, Jan. 2014.

[14] Z. Wu, Y. Chen, B. Zhao, X. Kang, and Y. Ding, "Review of weed detection methods based on computer vision," *Sensors*, vol. 21, no. 11, p. 3647, May 2021.

[15] F. López-Granados, "Weed detection for site-specific weed management: Mapping and real-time approaches," *Weed Res.*, vol. 51, no. 1, pp. 1–11, Feb. 2011.

[16] Y. Li, Z. Guo, F. Shuang, M. Zhang, and X. Li, "Key technologies of machine vision for weeding robots: A review and benchmark," *Comput. Electron. Agricult.*, vol. 196, May 2022, Art. no. 106880.

[17] M. H. Asad and A. Bais, "Crop and weed leaf area index mapping using multi-source remote and proximal sensing," *IEEE Access*, vol. 8, pp. 138179–138190, 2020.

[18] M. H. Asad and A. Bais, "Weed density estimation using semantic segmentation," in *Proc. Image Video Technol., Int. Workshops*. Sydney, NSW, Australia: Springer, Nov. 2020, pp. 162–171.

[19] H. S. Ullah, M. H. Asad, and A. Bais, "End to end segmentation of canola field images using dilated U-Net," *IEEE Access*, vol. 9, pp. 59741–59753, 2021.

[20] M. Das and A. Bais, "DeepVeg: Deep learning model for segmentation of weed, canola, and canola flea beetle damage," *IEEE Access*, vol. 9, pp. 119367–119380, 2021.

[21] K. Simonyan and A. Zisserman, "Very deep convolutional networks for large-scale image recognition," 2014, *arXiv:1409.1556*.

[22] G. Zhang, C. Koparan, M. R. Ahmed, K. Howatt, and X. Sun, "Weed and crop species classification using computer vision and deep learning technologies in greenhouse conditions," *J. Agricult. Food Res.*, vol. 9, Sep. 2022, Art. no. 100325.

[23] J. Barroso, J. McCallum, and D. Long, "Optical sensing of weed infestations at harvest," *Sensors*, vol. 17, no. 10, p. 2381, Oct. 2017.

[24] P. W. Nugent, J. A. Shaw, P. Jha, B. Scherrer, A. Donelick, and V. Kumar, "Discrimination of herbicide-resistant kochia with hyperspectral imaging," *J. Appl. Remote Sens.*, vol. 12, no. 1, 2018, Art. no. 016037.

[25] B. Scherrer, J. Sheppard, P. Jha, and J. A. Shaw, "Hyperspectral imaging and neural networks to classify herbicide-resistant weeds," *J. Appl. Remote Sens.*, vol. 13, no. 4, 2019, Art. no. 044516.

[26] A. Shirzadifar, S. Bajwa, J. Nowatzki, and A. Bazrafkan, "Field identification of weed species and glyphosate-resistant weeds using high resolution imagery in early growing season," *Biosystems Eng.*, vol. 200, pp. 200–214, Dec. 2020.

[27] T. D. Schwinghamer and R. C. Van Acker, "Emergence timing and persistence of kochia *(Kochia scoparia)*," *Weed Sci.*, vol. 56, no. 1, pp. 37–41, Jan. 2008.

[28] J. A. Dille, P. W. Stahlman, J. Du, P. W. Geier, J. D. Riffel, R. S. Currie, R. G. Wilson, G. M. Sbatella, P. Westra, A. R. Kniss, M. J. Moechnig, and R. M. Cole, "Kochia *(Kochia scoparia)* emergence profiles and seed persistence across the central great plains," *Weed Sci.*, vol. 65, no. 5, pp. 614–625, Sep. 2017.

[29] D. J. Sebastian, S. J. Nissen, P. Westra, D. L. Shaner, and G. Butters, "Influence of soil properties and soil moisture on the efficacy of indaziflam and flumioxazin on kochia scoparia L.," *Pest Manage. Sci.*, vol. 73, no. 2, pp. 444–451, 2017.

[30] B. Gul, R. Ansari, I. Aziz, and M. A. Khan, "Salt tolerance of Kochia scoparia: A new fodder crop for highly saline arid regions," *Pakistan J. Botany*, vol. 42, no. 4, pp. 2479–2487, 2010.

[31] N. S. Orlovsky, U. N. Japakova, I. Shulgina, and S. Volis, "Comparative study of seed germination and growth of *Kochia prostrata* and *Kochia scoparia* (Chenopodiaceae) under salinity," *J. Arid Environments*, vol. 75, no. 6, pp. 532–537, Jun. 2011.

[32] Planet Labs. (2022). *Understanding Planetscope Instruments*. [Online]. Available: https://developers.planet.com/docs/apis/data/sensors/

[33] Croptimistic Technology. (2023). *Capture, Assess, and Expand Your Understanding: Swatcam*. [Online]. Available: https://swatmaps.com/product/swat-cam/

[34] (2023). *Sentinel-2 Mission Guide*. [Online]. Available: https://sentinel.esa.int/web/sentinel/missions/sentinel-2

[35] V. Badrinarayanan, A. Kendall, and R. Cipolla, "SegNet: A deep convolutional encoder–decoder architecture for image segmentation," *IEEE Trans. Pattern Anal. Mach. Intell.*, vol. 39, no. 12, pp. 2481–2495, Dec. 2017.

[36] L.-C. Chen, G. Papandreou, I. Kokkinos, K. Murphy, and A. L. Yuille, "DeepLab: Semantic image segmentation with deep convolutional nets, atrous convolution, and fully connected CRFs," *IEEE Trans. Pattern Anal. Mach. Intell.*, vol. 40, no. 4, pp. 834–848, Apr. 2018.

[37] O. Ronneberger, P. Fischer, and T. Brox, "U-Net: Convolutional networks for biomedical image segmentation," in *Medical Image Computing and Computer-Assisted Intervention–MICCAI*. Munich, Germany: Springer, Oct. 2015, pp. 234–241.

[38] K. He, X. Zhang, S. Ren, and J. Sun, "Deep residual learning for image recognition," in *Proc. IEEE Conf. Comput. Vis. Pattern Recognit. (CVPR)*, Jun. 2016, pp. 770–778.

[39] M. B. Sahaai, G. R. Jothilakshmi, D. Ravikumar, R. Prasath, and S. Singh, "ResNet-50 based deep neural network using transfer learning for brain tumor classification," in *Proc. Int. Conf. RECENT Innov. Sci. Technol. (RIST)*, 2022, Art. no. 020014.

[40] M. D. Zeiler, "ADADELTA: An adaptive learning rate method," 2012, *arXiv:1212.5701*.

[41] (2023). *About Segments. AI*. [Online]. Available: https://segments.ai/about

[42] M. H. Asad and A. Bais, "Weed detection in canola fields using maximum likelihood classification and deep convolutional neural network," *Inf. Process. Agricult.*, vol. 7, no. 4, pp. 535–545, Dec. 2020.

[43] J. Long, E. Shelhamer, and T. Darrell, "Fully convolutional networks for semantic segmentation," in *Proc. IEEE Conf. Comput. Vis. Pattern Recognit. (CVPR)*, Jun. 2015, pp. 3431–3440.

[44] H. Zhao, J. Shi, X. Qi, X. Wang, and J. Jia, "Pyramid scene parsing network," in *Proc. IEEE Conf. Comput. Vis. Pattern Recognit. (CVPR)*, Jul. 2017, pp. 2881–2890.

[45] H. Steppuhn and K. Wall, "*Kochia scoparia* emergence from saline soil under various water regimes," *Rangeland Ecol. Manag.*, vol. 46, no. 6, pp. 533–538, 1993.

MUHAMMAD HAMZA ASAD (Student Member, IEEE) received the B.Sc. degree in electrical engineering from the University of Engineering and Technology Lahore, Lahore, Pakistan, in 2009, and the M.Sc. degree in electronic systems engineering from the University of Regina, SK, Canada, in 2019, where he is currently pursuing the Ph.D. degree in electronic systems engineering. His research interests include signal processing, machine learning, and artificial intelligence algorithms, with a special focus on precision agriculture. He is also working on applications of AI in variable rate technology in site-specific management of agriculture fields. It includes monitoring crops and weeds and mapping soil attributes, such as texture and organic matter.

SAJID SALEEM received the B.Sc. and M.Sc. degrees in electrical engineering from the University of Engineering and Technology Peshawar, Peshawar, Pakistan, in 2006 and 2009, respectively, and the Ph.D. degree from the Vienna Ph.D. School of Informatics, Vienna University of Technology, Austria, in 2014. With a strong record of publications in reputable conferences and journals, he has also served as a reviewer and a TPC member for various journals and international conferences. Currently, he is affiliated with the National University of Modern Languages, Islamabad, where he focuses his research on fields, such as communication signal processing, computer vision, image analysis, speech recognition, and deep learning.

ABDUL BAIS (Senior Member, IEEE) is currently an Associate Professor with the Faculty of Engineering and Applied Science, University of Regina. His research interests include deep learning, data analysis, image processing, and computer vision. His research is supported by the Natural Sciences and Engineering Research Council of Canada (NSERC Alliance and Discovery programs), Mitacs (www.mitacs.ca), the Saskatchewan Ministry of Agriculture, and the AgTech industry. He is a Certified Instructor with the NVIDIA Deep Learning Institute, and a Licensed Professional Engineer in Saskatchewan, Canada.

● ● ●